

Human Germline Heterozygous Gain-of-Function *STAT6* Variants Cause Severe Allergic Disease

Mehul Sharma^{1,2}, Henry Y. Lu^{1,2}, Maryam Vaseghi-Shanjani^{1,2}, Kate L. Del Bel¹, Oriol Fornes^{3,4}, Robin van der Lee^{3,4}, Phillip A. Richmond^{1,3}, Susan Lin¹, Joshua Dalmann¹, Jessica J. Lee^{3,5}, Allison Matthews³, Géraldine Blanchard-Rohner^{1,6}, Clara D M van Karnebeek^{3,7}, H. Melanie Bedford^{8,9}, Wyeth W. Wasserman³, Michael Seear¹, Margaret L. McKinnon⁴, Hanan Ahmed¹⁰, Stuart E. Turvey^{1,2}

¹Department of Pediatrics, BC Children's Hospital, The University of British Columbia, Vancouver, British Columbia, Canada

²Experimental Medicine Program, Faculty of Medicine, The University of British Columbia, British Columbia, Canada

³Centre for Molecular Medicine and Therapeutics, BC Children's Hospital Research Institute, Vancouver, BC, Canada

⁴Department of Medical Genetics, University of British Columbia, Vancouver, BC, Canada

⁵Genome Science and Technology Graduate Program, University of British Columbia, Vancouver, BC, Canada.

⁶Unit of Immunology and Vaccinology, Division of General Pediatrics, Department of Woman, Child, and Adolescent Medicine, Geneva University Hospitals and Faculty of Medicine, University of Geneva, Geneva, Switzerland.

⁷Departments of Pediatrics and Clinical Genetics, Amsterdam University Medical Centers, Amsterdam, The Netherlands

⁸Genetics Program, North York General Hospital, 4001 Leslie Street, Toronto, Ontario, Canada.

⁹Department of Paediatrics, University of Toronto, Toronto, Ontario, Canada.

¹⁰Faculty of Health Sciences, McMaster University, Hamilton, Ontario, Canada

Correspondence to: Stuart E. Turvey, MBBS, DPhil, FRCPC
BC Children's Hospital
950 West 28th Avenue
Vancouver, BC, V5Z 4H4, Canada
Phone: 604 875 2345 ext. 5094
Email: sturvey@cw.bc.ca

Running Title: Human germline *STAT6* gain-of-function variants

Word Count: 4439

Abstract Word Count: 209

Figure Count: 4

Reference Count: 98

40 **ABSTRACT**

41 STAT6 (Signal transducer and activator of transcription 6) is a transcription factor that
42 plays a central role in the pathophysiology of allergic inflammation. STAT6 mediates the
43 biological effects of IL-4, a cytokine necessary for type 2 differentiation of T cells and B
44 cell survival, proliferation and class switching to IgE. We have identified two
45 unrelated patients with a phenotype notable for their early-life onset of profound allergic
46 immune dysregulation, widespread treatment-resistant atopic dermatitis,
47 hypereosinophilia with eosinophilic esophagitis, elevated serum IgE, IgE-mediated
48 food allergies, and vascular anomalies of the brain. Both patients harbored
49 heterozygous *de novo* missense variants in the DNA binding domain of *STAT6*
50 (c.1144G>C, p.E382Q; and c.1256A>G, p.D419G). Functional studies established that
51 both variants caused a gain-of-function (GOF) phenotype associated with enhanced
52 phosphorylation and transcriptional activity of STAT6, in addition to increased transcript
53 abundance of known STAT6 target genes and other genes implicated in allergic
54 disease. JAK inhibitors decreased the enhanced STAT6 responses associated with
55 both these STAT6 GOF variants. This study identifies heterozygous GOF variants in
56 *STAT6* as a novel autosomal dominant allergic disorder. We anticipate that our
57 discovery of the first humans with germline *STAT6* GOF variants will facilitate the
58 recognition of more affected individuals and the full definition of this new primary atopic
59 disorder.

60

61 INTRODUCTION

62 Signal transducer and activator of transcription (STAT) proteins are a family of seven
63 mammalian transcription factors (STAT1, STAT2, STAT3, STAT4, STAT5A/B, and
64 STAT6) responsible for regulating the expression of genes involved in cellular immunity,
65 survival, proliferation, and differentiation^{1,2}. Although they each have unique functions,
66 they share sequence homology and possess similar activation mechanisms³. In
67 general, upon extracellular cytokine/growth factor-receptor engagement, intracellular
68 membrane receptor-associated Janus kinases (JAK) undergo transphosphorylation and
69 activation, leading to receptor tyrosine phosphorylation⁴. Phosphorylated tyrosine
70 residues on the receptor then create binding sites for the normally cytosolic-located Src
71 homology 2 (SH2) domain-containing STATs to bind and become phosphorylated and
72 activated. Phosphorylated STATs, dimerize and translocate into the nucleus, where
73 they bind to specific DNA sequences and regulate transcription⁴⁻⁷. As such, STATs are
74 critical for transducing extracellular cytokine-induced responses to transcriptional
75 changes in the nucleus.

76 Signal transducer and activator of transcription 6 (STAT6) is the main transcription
77 factor that mediates the biological effects of IL-4, a cytokine necessary for type 2
78 differentiation of T cells, as well as B cell survival, proliferation and class switching to
79 IgE⁸⁻¹¹. IL-4 is predominantly secreted by T cells, mast cells, basophils, and type 2
80 innate lymphoid cells¹². To mediate its effects, IL-4 binds the widely expressed IL-4R α
81 and this complex then binds secondary receptors chains¹³. In hematopoietic cells, the
82 secondary receptor chain is the common γ c chain also used by IL-2, IL-7, IL-9 and IL-15
83 and this forms the type 1 IL-4R system¹⁴. In non-hematopoietic cells such as epithelial
84 cells, the secondary receptor chain is IL-13R α , which forms the type 2 IL-4R system¹³.
85 Activation of these two receptor systems lead to diverse functions. In B cells, IL-4-
86 STAT6 signalling supports the growth and differentiation of B cells as well as secretion
87 of pro-allergic immunoglobulin E (IgE)⁹. In T cells, the IL-4-STAT6 axis is critical for the
88 differentiation of T helper 2 (T_H2) cells¹⁵, a subset of CD4⁺ helper T cells that is a major
89 contributor to the pathogenesis of allergic disease. In epithelial cells, the IL-4/IL-13-
90 STAT6 pathway has been implicated in barrier dysfunction^{16,17} and chronic pruritus¹⁸.

91 Collectively, the IL-4-STAT6 axis drives the development and progression of allergic
92 disease and asthma. Indeed, a monoclonal antibody directed against IL-4R α
93 (dupilumab) is clinically approved for treating allergic inflammation^{19,20}. Mouse studies
94 further emphasize the central role that STAT6 plays in the allergic diathesis. Mice
95 lacking STAT6 fail to develop many of the features of allergic inflammation²¹⁻²³.

96 In 2018, the term primary atopic disorders (PADs) was coined to describe heritable
97 genetic disorders presenting with dysregulated pathogenic allergic effector responses²⁴⁻
98 ²⁶. PADs are a subgroup of inborn errors of immunity (IEIs) that manifest with prominent
99 allergic inflammation, in the presence or absence of other clinical features associated
100 with IEIs, such as enhanced susceptibility to infections, autoimmunity, and malignancy.
101 Of the ~40 monogenic causes of PADs described to date, 12 impact the JAK-STAT
102 signaling cascade that is critical for cytokine responsiveness. For example, both loss-of-
103 function (LOF) and gain-of-function (GOF) variants in *STAT3*^{27,28} and *STAT5B*^{29,30}, and
104 GOF variants in *JAK1*^{31,32} and *STAT1*³³ cause PADs. Furthermore, defects in the genes
105 encoding upstream and downstream proteins in the STAT pathway (e.g. *ZNF341*,
106 *DOCK8*, *IL6ST*, *IL6R*, and *ERBIN*) also result in severe allergic diseases²⁶. The recent
107 increased recognition of PADs is valuable because: (i) the identification of affected
108 pathways provide important insights into the pathogenesis of allergic inflammation and
109 may uncover new treatment targets; (ii) these conditions are likely under-diagnosed
110 since allergies are traditionally believed to be complex polygenic disorders; and (iii)
111 diagnosis of PADs can be transformative for affected individuals and their families by
112 guiding treatment options, and informing relevant considerations tied to genetic
113 counselling including family planning, long term prognosis, and connection to other
114 families with the same genetic disease.

115 In this study, we describe a novel human PAD caused by germline heterozygous GOF
116 variants in the DNA binding domain of *STAT6* found in two unrelated individuals with
117 severe allergic disease and vascular anomalies of the brain.

118

119

120 **METHODS**

121 **Ethical Considerations:** All study participants provided written informed consent.
122 Research study protocols were approved by The University of British Columbia Clinical
123 Research Ethics Board.

124 **Identification of STAT6 variant via whole exome sequencing:** Trio whole exome
125 sequencing (WES) was performed as previously described³⁴. Briefly, WES was
126 performed on genomic DNA extracted from the first patient (P1) and both his parents
127 and a novel *de novo* predicted damaging STAT6 variant (c.1144G>C p.E382Q) was
128 selected for further analysis. WES was also performed on genomic DNA extracted from
129 the second patient (P2), her mother, and one of her brothers. A novel *de novo* predicted
130 damaging variant for STAT6 (c.1256A>G, p.D419G) was identified. Sanger sequencing
131 on saliva samples collected from the remaining family members of P2 revealed that no
132 other individuals carried the variant and that it segregates with disease.

133 **Generation of STAT6 variant plasmids:** Plasmids used for transfection studies
134 contained full-length STAT6 in a pCMV6 entry vector with a C-terminal GFP tag (Cat#:
135 RG210065, OriGene Technologies; Rockville, Maryland, USA). To generate p.E382Q
136 and p.D419G STAT6, a Q5 site-directed mutagenesis kit (Cat# E0554S, New England
137 Biolabs, Ipswich, MA, USA) was used according to manufacturer's recommendations
138 along with the following primer pairs: 5'-TGTCACAGAGCAGAAGTGCGC-3', 5'-
139 GACTCAGTGCCCTTCCGC-3', and 5'-GGCAACCAAGGCAACAATGCC-3', 5'-
140 ATGGACGATGACCACCAG-3', respectively.

141 To generate lentivirus vectors, wild type (WT), p.E382Q, and p.D419G STAT6 from the
142 above plasmids were cloned into a GFP-tagged Lenti vector (Cat#: PS100071, OriGene
143 Technologies, Rockville, MD, United States) using EcoRI-HF (Cat#: R3101) and NotI-
144 HF (Cat#: R3189) both from New England BioLabs. The three STAT6 plasmids were
145 packaged using 3rd generation packaging plasmids and transfected into HEK293T
146 cells. Culture media was collected, centrifuged, filtered, concentrated, and stored at -
147 80°C before use.

148 All new variant plasmids were confirmed by Sanger sequencing and purified from 10-
149 beta competent *E. coli* using a QIAprep Spin Miniprep Kit (Qiagen, ON, Canada).

150 **Transient and stable expression of STAT6 variants:** Transient expression of STAT6
151 variants in HEK293 cells were accomplished using a Lipofectamine 3000 kit (Thermo
152 Fisher Scientific, Waltham, MA, USA) according to manufacturer's recommendations.
153 Briefly, HEK293 cells were seeded at 8.0×10^5 cells/well in a 6-well plate in 1.5 mL of
154 Dulbecco modified Eagle medium (DMEM) with 10% FBS (Gibco, Life Technologies;
155 Rockville, MD, USA) and incubated for 24 hours at 37°C. Cells were transfected with
156 2.5µg of plasmid DNA using the P3000 and Lipofectamine 3000 reagents and harvested
157 after 24h.

158 Stable expression of STAT6 in Jurkat T cells was accomplished using the Lentivirus
159 approach as previously described^{35,36}. Briefly, Jurkat T cells were infected with lentiviral
160 particles in the presence of 5µg/ml polybrene (Sigma-Aldrich, St Louis, MO, USA) and
161 spinoculated at 800 x g for 30mins at 32°C, cultured, and expanded in complete RPMI-
162 1640 (GE Healthcare, Chicago, IL, United States) supplemented with 10% FBS.
163 Expanded cells were sorted on GFP expression using a BD FACS Aria (BD
164 Biosciences) cell sorter.

165 **Determining STAT6 variant activity by phospho-flow cytometry:** Phospho-STAT6
166 activity was quantified by flow cytometry in transfected cells stimulated with 100ng/mL
167 of IL-4 (Cat# 204-IL-020, R & D Systems, Minneapolis, MN, USA) for 1h or transfected
168 cells pre-treated with either 10µM ruxolitinib (Cat code: tlr-rux, Invivogen, San Diego,
169 CA, USA) or 4µM tofacitinib (Cat# S50001, Selleckchem, Houston, TX, USA) for 2h
170 before stimulation as previously described³⁷. Briefly, transfected and stimulated cells
171 were fixed using BD Cytofix (Cat# 554655, BD Biosciences, Ontario, Canada) for 20
172 min at 4°C and permeabilized using Perm III for 30 min on ice (Cat# 558050 BD
173 Biosciences). The cells were then stained with STAT6 PE-CF594 (Cat# 564148, BD
174 Biosciences) and p-STAT6 AF647 (Cat# 612601, BD Biosciences). pSTAT6 expression
175 was measured in GFP⁺STAT6⁺ cells from WT and STAT6 variants samples on an LSRII

176 flow cytometer (BD Biosciences) and analyzed using FlowJo software (BD
177 Biosciences).

178 **Luciferase reporter assays:** A luciferase reporter plasmid encoding a 4x STAT6
179 binding site [TTCCCAAGAA] was used to assess WT and variant STAT6 promoter
180 activity³⁸. The p4xSTAT6-Luc2P plasmid was a gift from Axel Nohturfft (Addgene
181 plasmid #35554; <http://n2t.net/addgene:35554>; RRID:Addgene_35554). Briefly, HEK293
182 cells were seeded in 24-well plates overnight at a density of 150k cells and transfected
183 with 250ng of p4xSTAT6-Luc2P, 250ng of a plasmid encoding GFP-tagged WT,
184 p.E382Q, or p.D419G *STAT6*, and 10ng Renilla luciferase (R-Luc) using lipofectamine
185 3000 as described above. Transfected cells were subsequently stimulated with
186 100ng/mL of IL-4 (Cat# 6507-IL-010, R&D Systems, Minneapolis, MN, USA) or left
187 untreated. Cell lysates were prepared and processed using a Dual-Glo Luciferase
188 Assay Kit (Cat#: E2920, Promega, Madison, WI, USA) according to manufacturer's
189 recommendations. Luciferase activity was measured on the Infinite M200 plate reader
190 (Tecan; Männedorf, Switzerland).

191 **RNA sequencing:** To investigate the global transcriptome, *STAT6* variant-transduced
192 Jurkat T cells were left unstimulated, or stimulated with 100ng/mL IL-4 for 4h. RNA was
193 extracted in triplicate as previously described³⁷ using a RNeasy Mini Plus Kit (Qiagen)
194 according to manufacturer's recommendations. RNA was prepared following the
195 standard protocol for the NEBNext Ultra II Stranded mRNA (New England Biolabs) and
196 sequenced on the Illumina NextSeq 500 with Paired End 42 bp × 42 bp reads. De-
197 multiplexed read sequences were aligned to a reference sequence using RNA-Seq
198 Alignment app (v1.1.1) on Illumina Basespace, using Spliced Transcripts Alignment to a
199 Reference (STAR) aligner and Cufflinks 2 for assembly and estimation of gene
200 expression.

201 Expression data were normalized to reads between samples using the edgeR package
202 in R (R Foundation, Vienna, Austria). Normalized counts were filtered to remove low
203 counts using the filterByExpr function in edgeR³⁹. Principal component analysis (PCA)
204 was done on $\log_2(\text{normalized counts}+0.25)$ in R using the PCA function. Differential

205 expression between unstimulated and stimulated samples for all three *STAT6*-
206 transduced Jurkat T cells was accomplished using Limma⁴⁰. Differentially expressed
207 genes were defined as those with fold change (FC) greater than 1.25 and adjusted p-
208 value less than 0.05.

209 Pathway analysis was done by first performing Gene Set Enrichment Analysis (GSEA)
210 with 1000 permutations using the Molecular Signatures Database Hallmark module.
211 Signal-to-noise ratio was used for gene ranking and the obtained NESs and P-values
212 were further adjusted using the Benjamini-Hochberg method. Pathways with an
213 adjusted P-value < 0.05 were considered significant. Leading edge genes from
214 significant pathways between *STAT6* WT and *STAT6* c.1256A>G Jurkat were identified
215 (no significantly upregulated pathways were identified between *STAT6* Wild Type and
216 *STAT6* c.1144G>C). Expression levels of these genes were then determined in each of
217 the three groups (Wild Type, c.1144G>C, c.1256A>G) under both stimulated and
218 unstimulated conditions. Sample level enrichment analyses (SLEA) scores were
219 computed as previously described⁴¹. Briefly, z-scores were computed for gene sets of
220 interest for each sample. The mean expression levels of significant genes were
221 compared to the expression of 1000 random gene sets of the same size. The difference
222 between observed and expected mean expression was then calculated and represented
223 on heatmaps.

224 Gene set enrichment analysis was also done on two other gene sets: i) *STAT6* targets;
225 and ii) IL-4 T_H2 targets. *STAT6* targets were defined as the set of genes that were
226 significantly upregulated upon IL-4 stimulation in WT-*STAT6* transduced Jurkat T cells.
227 Enrichment of this gene set was determined at both baseline and after IL-4 stimulation
228 between WT and p.E382Q *STAT6*, and WT and p.D419G *STAT6* Jurkat T cells. IL-4-
229 *STAT6* T_H2 skewing targets were previously reported⁴² *STAT6* target genes that are
230 significantly upregulated in response to IL-4 treatment and that lead to T_H2 skewing.

231 Raw data will be deposited on Gene Expression Omnibus.

232 **Structural modeling:** The effects of the *STAT6* variants on the protein function and
233 structure were analyzed using three-dimensional models. We used SWISS-MODEL⁴³ to

234 model the variants based on a template structure of the human STAT6 transcription
235 factor solved as a homodimer and in complex with DNA (PDB: 4Y5W, resolution: 3.1 Å,
236 chains A, C, M and N)³⁸. Structures were visualized with UCSF Chimera⁴⁴.

237

238

239 **RESULTS**

240 **Clinical features of two patients with severe atopic disease**

241 Patient A-II-1 (P1) was a male patient who had life-long severe allergic disease. The
242 patient was not dysmorphic and was born to unrelated parents. Soon after birth, P1
243 developed widespread, treatment-resistant atopic dermatitis (eczema),
244 gastroesophageal reflux with episodes of aspiration pneumonia, as well as chronic
245 diarrhea. He underwent Nissen fundoplication a few months later (with a surgical
246 revision in early childhood, age 6-10 years), following which gastrostomy feeding was
247 commenced. Over time, he was also diagnosed with multiple food and drug allergies
248 with anaphylactic reactions (combined with positive skin prick testing or RAST testing)
249 documented in response to peanuts, cows milk protein, bananas, sesame seeds, fish,
250 and eggs. He was fed with extensively hydrolyzed and elemental formulas via
251 gastrostomy with very limited oral feeding for much of his life. He was also diagnosed
252 with asthma. He experienced episodes of secondary bacterial skin infections from which
253 *Staphylococcus aureus*, group A streptococci and *Candida* spp. were isolated.
254 Widespread *molluscum contagiosum* was another notable skin finding. In his second
255 and third decade of life, he had persisting eczema, asthma, and perennial rhinitis which
256 worsened during pollen seasons. Repeated upper GI endoscopies confirmed the
257 diagnosis of eosinophilic esophagitis. During this time, most of his feeding consisted of
258 elemental formula via gastrostomy supplemented with limited oral intake (mainly rice,
259 potatoes, and chicken). He was treated with oral steroids for many years and
260 experienced symptom flares whenever the dose of prednisone was dropped below
261 10mg/day. He developed side-effects related to corticosteroids including cataracts,
262 osteoporosis, and pathogenic fractures. He had an episode of thromboembolic ischemia
263 of the right first and third toes with pain and cyanosis, ultimately requiring a lumbar
264 sympathectomy to relieve the pain. In his mid-30s (age 30-35 years), he was
265 hospitalized for non-bloody diarrhea, profound weight loss, malnutrition, weakness, and
266 vertigo. He was treated with high dose of prednisone, antibiotics, and elemental feeding.
267 During the hospitalization, he died after developing a spontaneous subarachnoid
268 hemorrhage with obstructive hydrocephalus, presumed secondary to an aneurysm

269 **(Table 1)**. Blood testing over the years confirmed eosinophilia and high serum IgE
270 levels **(Fig 1)**. Lymphocyte phenotyping and proliferation to a panel of mitogens were
271 found to be unremarkable when measured in early adulthood (ages 20-25 years). An
272 initial genetic assessment revealed normal sequences for *STAT3* and *DOCK8*,
273 prompting a more extensive genetic evaluation by WES.

274 Patient B-II-1 (P2) is a female who had similar life-long struggles with severe allergic
275 disease. She presented with severe chronic, treatment-resistant atopic dermatitis since
276 birth. She was diagnosed with IgE-mediated food allergy to egg, milk, peanut and tree
277 nuts early in life (age 0-5 years). She was diagnosed with asthma as an infant. In her
278 early life (age 0-5 years) she also had a pneumothorax requiring chest tube insertion,
279 required intubation for an asthma exacerbation, and was diagnosed with giant papillary
280 conjunctivitis which has remained an ongoing challenge. Other eye manifestations
281 included unilateral retinal detachment in her adolescence (age 15-20 years) and the
282 development of cataracts requiring surgery in early adulthood (age 20-25 years).
283 Through her second and third decades of life she continued to suffer from eczema,
284 asthma, recurrent bronchitis, rhinoconjunctivitis, and secondary staphylococcal and
285 candida skin infections. She had multiple dental abscess in the second and third
286 decades of her life. In her 20s she began experiencing gastrointestinal symptoms
287 culminating in biopsy diagnosed eosinophilic esophagitis and eosinophilic
288 gastroenteritis. Joint examination confirmed the presence of hypermobility. Serial blood
289 testing over the years confirmed eosinophilia and high serum IgE levels **(Fig 1)**. Brain
290 MRI in her mid-30s (ages 30-35 years) revealed multiple anatomical variants including
291 anomalous vasculature in the circle of Willis with hypoplastic vertebral arteries, a
292 persistent left-sided congenital trigeminal artery with tortuosity, and a hypoplastic A1
293 segment of the right anterior carotid artery **(Table 1)**. Multiple therapies were trialed
294 over the years with corticosteroids offering the most obvious benefits. To seek a
295 diagnosis for this spectrum of severe allergic manifestations, WES was performed on
296 the patient, her mother and one of her brothers.

297

298 **Whole-exome sequencing reveals novel *de novo* heterozygous variants in the**
299 **DNA binding domain of *STAT6***

300 The patients were found to carry heterozygous variants in the gene *STAT6*
301 (NM_001178079.2): c.1144G>C, p.E382Q for P1 and c.1256A>G, p.D419G for P2. The
302 variants were *de novo* as they were not found in any other family members (**Fig 1A**).
303 Both variants have not been reported in population databases (i.e. gnomAD), but
304 p.D419G can be found in the Catalogue of Somatic Mutations in Cancer (COSMIC)
305 database as a recurrent somatic variant in lymphoma with experimental evidence of a
306 GOF phenotype for this variant^{45,46}. Pathogenicity prediction models predict both
307 variants to be pathogenic, including CADD (Version 1.6, p.D419G: 29.3, p.E382Q:
308 27.7)⁴⁷, SIFT (p.D419G: 0.001, p.E382Q: 0.026)⁴⁸, and Polyphen-2 (p.D419G: 1.0,
309 p.E382Q: 1.0)⁴⁹ (**Supp Table 1**). Clinical laboratory tests showed that both patients had
310 eosinophilia and markedly elevated IgE (**Fig 1B-C**). Both variants localized to the highly
311 conserved DNA binding domain of *STAT6* (**Fig 1D**). Glu382 and Asp419 lie close to the
312 regions responsible for protein-DNA interaction³⁸. Both of these variants decrease the
313 electro-negativity of the protein near the DNA-binding interface (due to loss of glutamic
314 acid (E) and aspartic acid (D)), and are predicted to enhance *STAT6* binding to DNA
315 (**Fig 1E**). These variants did not affect *STAT6* protein expression as measured by flow
316 cytometry in transfected HEK293 cells (**Fig 1F-G**).

317

318 **p.E382Q and p.D419G *STAT6* variants lead to increased phosphorylation and**
319 **transcription activity of *STAT6* in HEK293 cells**

320 To assess the functional impact of the p.E382Q and p.D419G *STAT6* variants, we
321 selected HEK293 cells as our system, as these cells lack endogenous *STAT6* but
322 express other components of the IL-4R pathway (**Fig 2A**)⁵⁰. HEK293 cells were
323 transfected with wild-type (WT), p.E382Q, or p.D419G *STAT6* and the phosphorylation
324 status of *STAT6* was quantified by flow cytometry after 24h (**Fig 2B**). At baseline, we
325 observed significantly increased phosphorylated *STAT6* in cells expressing the
326 p.E382Q and p.D419G variants when compared to WT. IL-4 stimulation led to increased

327 phospho-STAT6 in all conditions, with the variant expressing cells maintaining
328 significantly higher phospho-STAT6 than WT (**Fig 2C**). To investigate whether
329 increased phosphorylation of STAT6 in both variants lead to increased STAT6
330 transcription factor activity, we conducted luciferase assays with a reporter plasmid
331 containing a canonical 4x STAT6 binding site, TTCCAAGAA in HEK293 cells³⁸. Both
332 p.E382Q and p.D419G STAT6 variants resulted in significantly higher promoter activity
333 at baseline (**Fig 2D**). However, there was no significant difference in promoter activity
334 after 4h IL-4 stimulation (**Fig 2D**). Together these data confirm a GOF phenotype
335 caused by both p.E382Q and p.D419G STAT6 variants.

336

337 **p.E382Q and p.D419G STAT6 variants exert a gain-of-function phenotype in** 338 **Jurkat T cells**

339 Given the increased promoter activity of the p.E382Q and p.D419G STAT6 variants, we
340 were interested in evaluating how this may impact the global transcriptome. As
341 transcriptomic studies on HEK293 cells after IL-4 stimulation have been challenging to
342 interpret⁴⁵, we stably expressed p.E382Q and p.D419G STAT6 by lentivirus
343 transduction in Jurkat T leukemia cells, which express endogenous STAT6 and serve
344 as a model of heterozygosity⁵¹. Here, we observed significantly higher phospho-STAT6-
345 positivity at baseline for the p.E382Q- cells but not p.D419G- cells, when compared to
346 WT (**Fig 3A**). However, there was no significant difference in phospho-STAT6 positivity
347 after IL-4 stimulation (**Fig 3A**).

348 Transcriptomically, WT-, p.E382Q-, and p.D419G-transduced cells clustered separately
349 from each other both at baseline and after stimulation with IL-4 (**Fig 3B**). This confirmed
350 that all variant cells were responsive to IL-4, and identified a unique transcriptomic
351 signature for each. Differential gene expression analysis revealed significantly
352 increased transcript abundance of known STAT6 target genes, including *IL4R*⁵², *CISH*⁴⁵
353 and *EPAS*⁴², and genes that have been implicated in atopic disease, including *XBP1*⁵³
354 and *TGFBR2*⁵⁴ in p.E382Q and p.D419G transduced cells when compared to WT
355 transduced controls (**Fig 3C-H**).

356 In response to IL-4 stimulation, we observed 54, 145, and 159 significantly upregulated
357 genes in WT-, p.E382Q-, and p.D419G-transduced Jurkat T cells, respectively (**Fig 3I,**
358 **Supp Fig 2A**). Interestingly, p.E382Q and p.D419G had 67 and 80 uniquely increased
359 hits, which did not overlap with WT, nor with each other. On the other hand, p.E382Q
360 and p.D419G had 108 and 54 uniquely downregulated genes (**Fig 3I, Supp Fig 2A**).
361 This suggests that the altered activity of both p.E382Q and p.D419G is not restricted to
362 enhanced activity on known STAT6 targets alone.

363 To further investigate the differential gene expression patterns, we performed gene set
364 enrichment analyses (GSEA). We first defined IL-4-STAT6 targets as genes that were
365 significantly upregulated in stimulated WT STAT6-transduced Jurkat T cells (**Supp**
366 **Table 2**). We found enrichment of these targets in both p.E382Q and p.D419G Jurkats
367 only at baseline (p.E382Q NES 1.34, adj-pvalue 0.084; p.D419G NES 1.83, adj-pvalue
368 <0.001), but not after IL-4 stimulation. Notably, after IL-4 stimulation both p.E382Q and
369 p.D419G STAT6 Jurkats showed significantly increased enrichment of IL-4 responsive
370 T_H2 skewing targets⁴² (p.E382Q NES 1.56, adj-pvalue <0.001; p.D419G NES 1.52, adj-
371 pvalue 0.007)(**Fig 3J**).

372 GSEA using the MSigDB Hallmark gene sets showed no significant difference in
373 enrichment in immunological pathways between WT and p.E382Q STAT6 both at
374 baseline and in response to stimulation (**Fig 3K, Supp Table 3**). However, p.D419G
375 STAT6 exhibited significantly increased enrichment in proliferation (Myc, G2M, DNA
376 repair, E2F) pathways, consistent with the fact that p.D419G (but not p.E382Q) is
377 reported as a recurrent somatic mutation in lymphoma^{45,55,56}, establishing this variant as
378 oncogenic.

379

380 **JAK inhibitors reduce enhanced STAT6 phosphorylation induced by p.E382Q and** 381 **p.D419G STAT6 in HEK293 cells**

382 Having demonstrated that both p.E382Q and p.D419G STAT6 are GOF variants, we
383 tested whether small molecule inhibitors that target the STAT6 pathway could

384 potentially be clinically beneficial. We selected JAK inhibitors, ruxolitinib and tofacitinib,
385 as both of these drugs are already used clinically for treating atopic disease^{57,58}. Both
386 inhibitors effectively decreased the enhanced STAT6 phosphorylation observed at
387 baseline and after IL-4 stimulation in cells expressing the p.E382Q or p.D419G STAT6
388 variants (**Fig 4A-B**). This suggests that JAK inhibitors may be promising treatment
389 options for patients with GOF *STAT6* variants.

390

391

392 **DISCUSSION**

393 In this study, we present a combination of clinical, molecular, and transcriptional
394 evidence of a new human disorder caused by germline autosomal dominant GOF
395 *STAT6* variants in two patients with life-long severe allergic disease. These variants led
396 to increased *STAT6* phosphorylation, increased *STAT6* target gene expression, and
397 T_H2 skewed transcriptional profile. Although the full phenotype of GOF *STAT6* variants
398 will only be uncovered through the identification of additional affected individuals, we
399 propose to classify human germline autosomal dominant GOF *STAT6* syndrome as a
400 novel primary atopic disorder²⁴⁻²⁶. Based on our study, possible clinical ‘red flags’ for
401 this new disorder include: (i) early life onset; (ii) peripheral blood eosinophilia, (iii)
402 elevated serum IgE, (iii) widespread, treatment-resistant atopic dermatitis, (iv) multiple
403 food and drug allergies; (v) recurrent skin and respiratory infections; (vi) eosinophilic
404 gastrointestinal disorder, including eosinophilic esophagitis; (vii) allergic
405 rhinoconjunctivitis; and (viii) vascular malformations of the brain.

406 *STAT6* is intimately linked to the biology of allergic inflammation. The central and most
407 studied role of *STAT6* is in mediating the biological effects of IL-4, a cytokine necessary
408 for T_H2 differentiation, B cell survival, proliferation and class switching to IgE^{9,42}, and
409 driving M2 macrophage polarization⁵⁹. In T cells, *STAT6* activation induces the
410 expression of GATA3, the master regulator of T_H2 differentiation, which in turn
411 enhances expression of IL-4, IL-5 and IL-13, cytokines necessary for promoting allergic
412 responses by activating mast cells and eosinophils⁶⁰. Presence of greater T_H2 cell
413 populations, or T_H2 cells producing copious amounts of IL-4/IL-5/IL-13, could be a driver
414 of the observed allergic phenotype presented in our patients. Elevated IgE in
415 partnership with mast cells is important for both acute and chronic manifestations of
416 allergic disorders and can be an additional driver of the allergic diathesis⁶¹. *STAT6*
417 hyperactivation in airway epithelial cells and resident dendritic cells can further create
418 an environment favouring asthma and chronic lung disease, as this would induce
419 production of chemokines that promote T_H2 cells and eosinophil recruitment^{62,63}.
420 Population genetics provide further support for the central role that *STAT6* plays in the
421 development of human allergic disease. Multiple independent genome wide association

422 studies (GWAS) have found that polymorphisms in *STAT6* associate with many allergic
423 conditions (**Table 2**). Our study further expands this appreciation of the role of *STAT6* in
424 human disease by establishing that heterozygous GOF variants cause a monogenic
425 form of severe allergic disease.

426 The fatal cerebral aneurysm in P1 (p.E382Q) was not clinically anticipated, but it is
427 possible that the *STAT6* GOF variant also increased the risk of developing cerebral
428 aneurysms. Intracranial aneurysms have been reported in patients with both *STAT3*
429 LOF and *STAT1* GOF⁶⁴⁻⁶⁶. Increased activation of other STAT family members,
430 including *STAT2*, *STAT3* and *STAT5* have also been observed in human abdominal
431 aortic aneurysms (*STAT6* was not evaluated), although it is not clear whether enhanced
432 STAT phosphorylation contributes to aneurysms or is the result of inflammation caused
433 by aneurysms⁶⁷. As more individuals with *STAT6* GOF variants are identified, the
434 possibility of cerebral vascular anomalies warrants investigation.

435 A GOF *STAT6* model (designated *STAT6VT*) has previously been described *in vitro*⁶⁸
436 and has been used to study chronic atopic dermatitis in mouse models^{69,70}. *STAT6VT*
437 has the substitution of two amino acid residues, at positions 547 and 548, in the SH2
438 domain resulting in a *STAT6* mutant that is constitutively active in an IL-4 independent
439 manner and is unresponsive to IL-4 stimulation⁶⁸. *STAT6VT* differs from the variants we
440 describe as the latter are in the DNA binding domain (**Fig 1**) and do respond to IL-4
441 stimulation (**Fig 2-4**). Nevertheless, the humans we identified with *STAT6* GOF variants
442 and *STAT6VT* mice share a number of key features of the allergic diathesis, including
443 elevated serum IgE and chronic atopic dermatitis.

444 There is now a growing list of human single gene defects that cause the classic hyper-
445 IgE phenotypic triad of eczema, recurrent skin and lung infections, and elevated serum
446 IgE^{26,71}. Autosomal dominant hyper-IgE syndrome caused by dominant negative
447 variants in *STAT3* (aka. Job's syndrome or *STAT3* LOF) is the best characterized of
448 these conditions, but this list of disorders does include both autosomal dominant
449 (*STAT3*, *CARD11*, *ERBIN*) and autosomal recessive (*DOCK8*, *PGM3*, *IL6ST*)
450 conditions^{72,73}. Notably, the patients we identified with *STAT6* GOF variants did have

451 some of the extra-immunological features typical of STAT3 LOF (i.e. hyperextensible
452 joints, fractures, vascular anomalies⁷³).

453 Based on the findings reported in this study, we suggest that heterozygous GOF
454 variants in STAT6 be added to the list of autosomal dominant causes of the hyper-IgE
455 phenotype. While each of the conditions known to cause a hyper-IgE phenotype has
456 some specific clinical features (e.g. viral skin infections are a defining feature of DOCK8
457 deficiency^{74,75}), there is considerable clinical overlap and clinically-approved testing of
458 these pathways is rarely available. Therefore, we recommend genetic testing as the
459 most efficient initial diagnostic approach to patients who experience severe allergic
460 disease beginning very early in life. Finally, in common with other primary atopic
461 disorders³¹, we demonstrate that JAK inhibition may be an effective treatment for
462 patients with GOF *STAT6* variants.

463 While this study has many strengths, notably the extreme allergic phenotype of the two
464 patients combined with in-depth functional assessment of their *de novo* *STAT6* variants,
465 a limitation is our lack of validation in primary patient cells due to the death of P1 and
466 challenges with phlebotomy in P2 due to the severity of her atopic dermatitis. Despite
467 this limitation, our study does identify GOF variants in *STAT6* as a novel monogenic
468 allergic disorder. We anticipate that this discovery will facilitate the recognition of more
469 affected individuals and, with time, a full definition of the human phenotype caused by
470 germline human *STAT6* GOF variants will emerge.

471

472

473

474

475

476

477

478 **Acknowledgements:** This work was supported by grants from the Canadian Institutes
479 of Health Research (PJT 178054) (S.E.T.), Genome British Columbia (SIP007) (S.E.T.),
480 and BC Children’s Hospital Foundation. S.E.T. holds a Tier 1 Canada Research Chair in
481 Pediatric Precision Health and the Aubrey J. Tingle Professor of Pediatric Immunology.
482 M.S. is supported by a CIHR Frederick Banting and Charles Best Canada Graduate
483 Scholarships Doctoral Award (CGS-D) and University of British Columbia Four Year
484 Doctoral Fellowship (4YF). H.Y.L. is supported by a CGS-D, 4YF, Killam Doctoral
485 Scholarship, Friedman Award for Scholars in Health, and a BC Children’s Hospital
486 Research Institute Graduate Studentship. M.V.S. is funded by the Vanier Canada
487 Graduate Scholarship and the University of British Columbia 4-Year Doctoral Fellowship
488 (4YF). We would also like to acknowledge the Biomedical Research Centre Sequencing
489 Core (BRC-Seq) for their assistance with RNA-Sequencing and processing.

490

491 **Contribution:** Me.S., G.B.R, H.M.B, Mi.S, M.L.M, H.A, K.L.D., and S.E.T enrolled
492 patients and analyzed clinical data; J.J.L, A.M, W.W.W., C.D.M.v.K conducted genetic
493 screening and identified variants of significance. M.S., O.F, R.v.d.L, and P.A.R
494 performed, structural modeling, bioinformatic and statistical analysis; M.S., H.Y.L.,
495 M.V.S, K.L.D, S.L., and J.D. performed the laboratory experiments; M.S., H.Y.L., M.V.S,
496 and S.E.T. wrote and edited the manuscript. All authors reviewed the final manuscript.

497

498 **Conflict of Interest Disclosures:** Authors report no conflicts of interest in relation to
499 this manuscript.

500 **REFERENCES**

- 501 1. O'Shea JJ, Plenge R. JAK and STAT signaling molecules in immunoregulation
502 and immune-mediated disease. *Immunity* 2012;36:542-50.
- 503 2. Luo Y, Alexander M, Gadina M, O'Shea JJ, Meylan F, Schwartz DM. JAK-STAT
504 signaling in human disease: From genetic syndromes to clinical inhibition. *J Allergy Clin*
505 *Immunol* 2021;148:911-25.
- 506 3. Jatiani SS, Baker SJ, Silverman LR, Reddy EP. Jak/STAT pathways in cytokine
507 signaling and myeloproliferative disorders: approaches for targeted therapies. *Genes*
508 *Cancer* 2010;1:979-93.
- 509 4. Villarino AV, Kanno Y, Ferdinand JR, O'Shea JJ. Mechanisms of Jak/STAT
510 signaling in immunity and disease. *J Immunol* 2015;194:21-7.
- 511 5. Ihle JN. Cytokine receptor signalling. *Nature* 1995;377:591-4.
- 512 6. Mogensen TH. IRF and STAT Transcription Factors - From Basic Biology to
513 Roles in Infection, Protective Immunity, and Primary Immunodeficiencies. *Front*
514 *Immunol* 2018;9:3047.
- 515 7. Briscoe J, Guschin D, Rogers NC, et al. JAKs, STATs and signal transduction in
516 response to the interferons and other cytokines. *Philos Trans R Soc Lond B Biol Sci*
517 1996;351:167-71.
- 518 8. Goenka S, Kaplan MH. Transcriptional regulation by STAT6. *Immunologic*
519 *research* 2011;50:87-96.
- 520 9. Takeda K, Tanaka T, Shi W, et al. Essential role of Stat6 in IL-4 signalling.
521 *Nature* 1996;380:627-30.
- 522 10. Villarino AV, Kanno Y, O'Shea JJ. Mechanisms and consequences of Jak-STAT
523 signaling in the immune system. *Nat Immunol* 2017;18:374-84.
- 524 11. Villarino AV, Gadina M, O'Shea JJ, Kanno Y. Snapshot: Jak-STAT Signaling II.
525 *Cell* 2020;181:1696-.e1.
- 526 12. Mjosberg J, Bernink J, Golebski K, et al. The transcription factor GATA3 is
527 essential for the function of human type 2 innate lymphoid cells. *Immunity* 2012;37:649-
528 59.
- 529 13. Junttila IS. Tuning the Cytokine Responses: An Update on Interleukin (IL)-4 and
530 IL-13 Receptor Complexes. *Front Immunol* 2018;9:888.
- 531 14. Spolski R, Gromer D, Leonard WJ. The gamma c family of cytokines: fine-tuning
532 signals from IL-2 and IL-21 in the regulation of the immune response. *F1000Res*
533 2017;6:1872.
- 534 15. Kaplan MH, Schindler U, Smiley ST, Grusby MJ. Stat6 is required for mediating
535 responses to IL-4 and for development of Th2 cells. *Immunity* 1996;4:313-9.
- 536 16. Saatian B, Rezaee F, Desando S, et al. Interleukin-4 and interleukin-13 cause
537 barrier dysfunction in human airway epithelial cells. *Tissue Barriers* 2013;1:e24333.
- 538 17. Mannon P, Reinisch W. Interleukin 13 and its role in gut defence and
539 inflammation. *Gut* 2012;61:1765-73.
- 540 18. Oetjen LK, Mack MR, Feng J, et al. Sensory Neurons Co-opt Classical Immune
541 Signaling Pathways to Mediate Chronic Itch. *Cell* 2017;171:217-28 e13.
- 542 19. Bacharier LB, Maspero JF, Katelaris CH, et al. Dupilumab in Children with
543 Uncontrolled Moderate-to-Severe Asthma. *N Engl J Med* 2021;385:2230-40.
- 544 20. Beck LA, Thaci D, Hamilton JD, et al. Dupilumab treatment in adults with
545 moderate-to-severe atopic dermatitis. *N Engl J Med* 2014;371:130-9.

- 546 21. Tomkinson A, Kanehiro A, Rabinovitch N, Joetham A, Cieslewicz G, Gelfand
547 EW. The failure of STAT6-deficient mice to develop airway eosinophilia and airway
548 hyperresponsiveness is overcome by interleukin-5. *Am J Respir Crit Care Med*
549 1999;160:1283-91.
- 550 22. Akimoto T, Numata F, Tamura M, et al. Abrogation of bronchial eosinophilic
551 inflammation and airway hyperreactivity in signal transducers and activators of
552 transcription (STAT)6-deficient mice. *J Exp Med* 1998;187:1537-42.
- 553 23. Kuperman D, Schofield B, Wills-Karp M, Grusby MJ. Signal transducer and
554 activator of transcription factor 6 (Stat6)-deficient mice are protected from antigen-
555 induced airway hyperresponsiveness and mucus production. *J Exp Med* 1998;187:939-
556 48.
- 557 24. Lyons JJ, Milner JD. Primary atopic disorders. *J Exp Med* 2018;215:1009-22.
- 558 25. Milner JD. Primary Atopic Disorders. *Annu Rev Immunol* 2020;38:785-808.
- 559 26. Vaseghi-Shanjani M, Smith KL, Sara RJ, et al. Inborn errors of immunity
560 manifesting as atopic disorders. *J Allergy Clin Immunol* 2021;148:1130-9.
- 561 27. Asano T, Khourieh J, Zhang P, et al. Human STAT3 variants underlie autosomal
562 dominant hyper-IgE syndrome by negative dominance. *J Exp Med* 2021;218.
- 563 28. Fabre A, Marchal S, Barlogis V, et al. Clinical Aspects of STAT3 Gain-of-
564 Function Germline Mutations: A Systematic Review. *J Allergy Clin Immunol Pract*
565 2019;7:1958-69 e9.
- 566 29. Ma CA, Xi L, Cauff B, et al. Somatic STAT5b gain-of-function mutations in early
567 onset nonclonal eosinophilia, urticaria, dermatitis, and diarrhea. *Blood* 2017;129:650-3.
- 568 30. Kanai T, Jenks J, Nadeau KC. The STAT5b Pathway Defect and Autoimmunity.
569 *Front Immunol* 2012;3:234.
- 570 31. Del Bel KL, Ragotte RJ, Saferali A, et al. JAK1 gain-of-function causes an
571 autosomal dominant immune dysregulatory and hypereosinophilic syndrome. *J Allergy*
572 *Clin Immunol* 2017;139:2016-20 e5.
- 573 32. Gruber CN, Calis JJA, Buta S, et al. Complex Autoinflammatory Syndrome
574 Unveils Fundamental Principles of JAK1 Kinase Transcriptional and Biochemical
575 Function. *Immunity* 2020;53:672-84 e11.
- 576 33. Uzel G, Sampaio EP, Lawrence MG, et al. Dominant gain-of-function STAT1
577 mutations in FOXP3 wild-type immune dysregulation-polyendocrinopathy-enteropathy-
578 X-linked-like syndrome. *J Allergy Clin Immunol* 2013;131:1611-23.
- 579 34. Sharma M, Fu MP, Lu HY, et al. Human germline biallelic complete NFAT1
580 deficiency causes the triad of progressive joint contractures, osteochondromas, and
581 susceptibility to B cell malignancy. *medRxiv* 2022:2022.01.30.22269378.
- 582 35. Fung SY, Lu HY, Sharma M, et al. MALT1-Dependent Cleavage of HOIL1
583 Modulates Canonical NF-kappaB Signaling and Inflammatory Responsiveness. *Front*
584 *Immunol* 2021;12:749794.
- 585 36. Kutner RH, Zhang XY, Reiser J. Production, concentration and titration of
586 pseudotyped HIV-1-based lentiviral vectors. *Nat Protoc* 2009;4:495-505.
- 587 37. Lu HY, Sharma M, Sharma AA, et al. Mechanistic understanding of the combined
588 immunodeficiency in complete human CARD11 deficiency. *J Allergy Clin Immunol* 2021.
- 589 38. Li J, Rodriguez JP, Niu F, et al. Structural basis for DNA recognition by STAT6.
590 *Proc Natl Acad Sci U S A* 2016;113:13015-20.

- 591 39. Chen Y, Lun AT, Smyth GK. From reads to genes to pathways: differential
592 expression analysis of RNA-Seq experiments using Rsubread and the edgeR quasi-
593 likelihood pipeline. *F1000Res* 2016;5:1438.
- 594 40. Ritchie ME, Phipson B, Wu D, et al. limma powers differential expression
595 analyses for RNA-sequencing and microarray studies. *Nucleic Acids Res* 2015;43:e47.
- 596 41. Kulpa DA, Talla A, Brehm JH, et al. Differentiation into an Effector Memory
597 Phenotype Potentiates HIV-1 Latency Reversal in CD4(+) T Cells. *J Virol* 2019;93.
- 598 42. Elo LL, Jarvenpaa H, Tuomela S, et al. Genome-wide profiling of interleukin-4
599 and STAT6 transcription factor regulation of human Th2 cell programming. *Immunity*
600 2010;32:852-62.
- 601 43. Waterhouse A, Bertoni M, Bienert S, et al. SWISS-MODEL: homology modelling
602 of protein structures and complexes. *Nucleic Acids Res* 2018;46:W296-W303.
- 603 44. Pettersen EF, Goddard TD, Huang CC, et al. UCSF Chimera--a visualization
604 system for exploratory research and analysis. *J Comput Chem* 2004;25:1605-12.
- 605 45. Yildiz M, Li H, Bernard D, et al. Activating STAT6 mutations in follicular
606 lymphoma. *Blood* 2015;125:668-79.
- 607 46. Zamo A, Pischmarov J, Horn H, Ott G, Rosenwald A, Leich E. The exomic
608 landscape of t(14;18)-negative diffuse follicular lymphoma with 1p36 deletion. *Br J*
609 *Haematol* 2018;180:391-4.
- 610 47. Rentzsch P, Schubach M, Shendure J, Kircher M. CADD-Splice-improving
611 genome-wide variant effect prediction using deep learning-derived splice scores.
612 *Genome Med* 2021;13:31.
- 613 48. Sim NL, Kumar P, Hu J, Henikoff S, Schneider G, Ng PC. SIFT web server:
614 predicting effects of amino acid substitutions on proteins. *Nucleic Acids Res*
615 2012;40:W452-7.
- 616 49. Adzhubei IA, Schmidt S, Peshkin L, et al. A method and server for predicting
617 damaging missense mutations. *Nat Methods* 2010;7:248-9.
- 618 50. Mikita T, Campbell D, Wu P, Williamson K, Schindler U. Requirements for
619 interleukin-4-induced gene expression and functional characterization of Stat6. *Mol Cell*
620 *Biol* 1996;16:5811-20.
- 621 51. Kim Y, Kwon EK, Jeon JH, et al. Activation of the STAT6 transcription factor in
622 Jurkat T-cells by the herpesvirus saimiri Tip protein. *J Gen Virol* 2012;93:330-40.
- 623 52. Goenka S, Kaplan MH. Transcriptional regulation by STAT6. *Immunol Res*
624 2011;50:87-96.
- 625 53. Bettigole SE, Lis R, Adoro S, et al. The transcription factor XBP1 is selectively
626 required for eosinophil differentiation. *Nat Immunol* 2015;16:829-37.
- 627 54. Frischmeyer-Guerrerio PA, Guerrerio AL, Oswald G, et al. TGFbeta receptor
628 mutations impose a strong predisposition for human allergic disease. *Sci Transl Med*
629 2013;5:195ra94.
- 630 55. Tate JG, Bamford S, Jubb HC, et al. COSMIC: the Catalogue Of Somatic
631 Mutations In Cancer. *Nucleic Acids Res* 2019;47:D941-D7.
- 632 56. Ritz O, Guiter C, Castellano F, et al. Recurrent mutations of the STAT6 DNA
633 binding domain in primary mediastinal B-cell lymphoma. *Blood* 2009;114:1236-42.
- 634 57. Bissonnette R, Papp KA, Poulin Y, et al. Topical tofacitinib for atopic dermatitis: a
635 phase IIa randomized trial. *Br J Dermatol* 2016;175:902-11.

- 636 58. Kim BS, Howell MD, Sun K, et al. Treatment of atopic dermatitis with ruxolitinib
637 cream (JAK1/JAK2 inhibitor) or triamcinolone cream. *J Allergy Clin Immunol*
638 2020;145:572-82.
- 639 59. Ginhoux F, Schultze JL, Murray PJ, Ochando J, Biswas SK. New insights into the
640 multidimensional concept of macrophage ontogeny, activation and function. *Nat*
641 *Immunol* 2016;17:34-40.
- 642 60. Sloka S, Silva C, Wang J, Yong VW. Predominance of Th2 polarization by
643 vitamin D through a STAT6-dependent mechanism. *J Neuroinflammation* 2011;8:56.
- 644 61. Galli SJ, Tsai M. IgE and mast cells in allergic disease. *Nat Med* 2012;18:693-
645 704.
- 646 62. Matsukura S, Stellato C, Georas SN, et al. Interleukin-13 upregulates eotaxin
647 expression in airway epithelial cells by a STAT6-dependent mechanism. *Am J Respir*
648 *Cell Mol Biol* 2001;24:755-61.
- 649 63. Medoff BD, Seung E, Hong S, et al. CD11b+ myeloid cells are the key mediators
650 of Th2 cell homing into the airway in allergic inflammation. *J Immunol* 2009;182:623-35.
- 651 64. Chandesris MO, Azarine A, Ong KT, et al. Frequent and widespread vascular
652 abnormalities in human signal transducer and activator of transcription 3 deficiency. *Circ*
653 *Cardiovasc Genet* 2012;5:25-34.
- 654 65. Dadak M, Jacobs R, Skuljec J, et al. Gain-of-function STAT1 mutations are
655 associated with intracranial aneurysms. *Clin Immunol* 2017;178:79-85.
- 656 66. Toubiana J, Okada S, Hiller J, et al. Heterozygous STAT1 gain-of-function
657 mutations underlie an unexpectedly broad clinical phenotype. *Blood* 2016;127:3154-64.
- 658 67. Liao M, Xu J, Clair AJ, Ehrman B, Graham LM, Eagleton MJ. Local and systemic
659 alterations in signal transducers and activators of transcription (STAT) associated with
660 human abdominal aortic aneurysms. *J Surg Res* 2012;176:321-8.
- 661 68. Daniel C, Salvekar A, Schindler U. A gain-of-function mutation in STAT6. *J Biol*
662 *Chem* 2000;275:14255-9.
- 663 69. DaSilva-Arnold SC, Thyagarajan A, Seymour LJ, et al. Phenotyping acute and
664 chronic atopic dermatitis-like lesions in Stat6^{VT} mice identifies a role for IL-33 in
665 disease pathogenesis. *Arch Dermatol Res* 2018;310:197-207.
- 666 70. Bruns HA, Schindler U, Kaplan MH. Expression of a constitutively active Stat6 in
667 vivo alters lymphocyte homeostasis with distinct effects in T and B cells. *J Immunol*
668 2003;170:3478-87.
- 669 71. Freeman AF, Milner JD. The Child with Elevated IgE and Infection Susceptibility.
670 *Curr Allergy Asthma Rep* 2020;20:65.
- 671 72. Minegishi Y. Hyper-IgE syndrome, 2021 update. *Allergol Int* 2021;70:407-14.
- 672 73. Bergerson JRE, Freeman AF. An Update on Syndromes with a Hyper-IgE
673 Phenotype. *Immunol Allergy Clin North Am* 2019;39:49-61.
- 674 74. Biggs CM, Keles S, Chatila TA. DOCK8 deficiency: Insights into pathophysiology,
675 clinical features and management. *Clin Immunol* 2017;181:75-82.
- 676 75. Chu EY, Freeman AF, Jing H, et al. Cutaneous manifestations of DOCK8
677 deficiency syndrome. *Arch Dermatol* 2012;148:79-84.
- 678 76. Sakaue S, Kanai M, Tanigawa Y, et al. A cross-population atlas of genetic
679 associations for 220 human phenotypes. *Nature Genetics* 2021;53:1415-24.

- 680 77. Zhu Z, Guo Y, Shi H, et al. Shared genetic and experimental links between
681 obesity-related traits and asthma subtypes in UK Biobank. *Journal of Allergy and*
682 *Clinical Immunology* 2020;145:537-49.
- 683 78. Pividori M, Schoettler N, Nicolae DL, Ober C, Im HK. Shared and distinct genetic
684 risk factors for childhood-onset and adult-onset asthma: genome-wide and
685 transcriptome-wide studies. *The Lancet Respiratory Medicine* 2019;7:509-22.
- 686 79. Ferreira MAR, Mathur R, Vonk JM, et al. Genetic Architectures of Childhood- and
687 Adult-Onset Asthma Are Partly Distinct. *The American Journal of Human Genetics*
688 2019;104:665-84.
- 689 80. Zhu Z, Lee PH, Chaffin MD, et al. A genome-wide cross-trait analysis from UK
690 Biobank highlights the shared genetic architecture of asthma and allergic diseases.
691 *Nature Genetics* 2018;50:857-64.
- 692 81. Johansson Å, Rask-Andersen M, Karlsson T, Ek WE. Genome-wide association
693 analysis of 350 000 Caucasians from the UK Biobank identifies novel loci for asthma,
694 hay fever and eczema. *Human Molecular Genetics* 2019;28:4022-41.
- 695 82. Zhu Z, Zhu X, Liu C-L, et al. Shared genetics of asthma and mental health
696 disorders: a large-scale genome-wide cross-trait analysis. *European Respiratory*
697 *Journal* 2019;54:1901507.
- 698 83. Demenais F, Margaritte-Jeannin P, Barnes KC, et al. Multiancestry association
699 study identifies new asthma risk loci that colocalize with immune-cell enhancer marks.
700 *Nature Genetics* 2018;50:42-53.
- 701 84. Pickrell JK, Berisa T, Liu JZ, Séguérel L, Tung JY, Hinds DA. Detection and
702 interpretation of shared genetic influences on 42 human traits. *Nature Genetics*
703 2016;48:709-17.
- 704 85. Shrine N, Portelli MA, John C, et al. Moderate-to-severe asthma in individuals of
705 European ancestry: a genome-wide association study. *The Lancet Respiratory Medicine*
706 2019;7:20-34.
- 707 86. Valette K, Li Z, Bon-Baret V, et al. Prioritization of candidate causal genes for
708 asthma in susceptibility loci derived from UK Biobank. *Communications Biology* 2021;4.
- 709 87. Olafsdottir TA, Theodors F, Bjarnadottir K, et al. Eighty-eight variants highlight
710 the role of T cell regulation and airway remodeling in asthma pathogenesis. *Nature*
711 *Communications* 2020;11.
- 712 88. Han Y, Jia Q, Jahani PS, et al. Genome-wide analysis highlights contribution of
713 immune system pathways to the genetic architecture of asthma. *Nature*
714 *Communications* 2020;11.
- 715 89. Astle WJ, Elding H, Jiang T, et al. The Allelic Landscape of Human Blood Cell
716 Trait Variation and Links to Common Complex Disease. *Cell* 2016;167:1415-29.e19.
- 717 90. Vuckovic D, Bao EL, Akbari P, et al. The Polygenic and Monogenic Basis of
718 Blood Traits and Diseases. *Cell* 2020;182:1214-31.e11.
- 719 91. Kachuri L, Jeon S, Dewan AT, et al. Genetic determinants of blood-cell traits
720 influence susceptibility to childhood acute lymphoblastic leukemia. *The American*
721 *Journal of Human Genetics* 2021;108:1823-35.
- 722 92. Chen M-H, Raffield LM, Mousas A, et al. Trans-ethnic and Ancestry-Specific
723 Blood-Cell Genetics in 746,667 Individuals from 5 Global Populations. *Cell*
724 2020;182:1198-213.e14.

- 725 93. Kichaev G, Bhatia G, Loh P-R, et al. Leveraging Polygenic Functional
726 Enrichment to Improve GWAS Power. *The American Journal of Human Genetics*
727 2019;104:65-75.
- 728 94. Ferreira MAR, Vonk JM, Baurecht H, et al. Age-of-onset information helps
729 identify 76 genetic variants associated with allergic disease. *PLOS Genetics*
730 2020;16:e1008725.
- 731 95. Ferreira MA, Vonk JM, Baurecht H, et al. Shared genetic origin of asthma, hay
732 fever and eczema elucidates allergic disease biology. *Nature Genetics* 2017;49:1752-7.
- 733 96. Tanaka N, Koido M, Suzuki A, et al. Eight novel susceptibility loci and putative
734 causal variants in atopic dermatitis. *Journal of Allergy and Clinical Immunology*
735 2021;148:1293-306.
- 736 97. Granada M, Wilk JB, Tuzova M, et al. A genome-wide association study of
737 plasma total IgE concentrations in the Framingham Heart Study. *Journal of Allergy and*
738 *Clinical Immunology* 2012;129:840-5.e21.
- 739 98. Daya M, Cox C, Acevedo N, et al. Multiethnic genome-wide and HLA association
740 study of total serum IgE level. *Journal of Allergy and Clinical Immunology*
741 2021;148:1589-95.
- 742 99. Waage J, Standl M, Curtin JA, et al. Genome-wide association and HLA fine-
743 mapping studies identify risk loci and genetic pathways underlying allergic rhinitis.
744 *Nature Genetics* 2018;50:1072-80.
- 745 100. Bønnelykke K, Matheson MC, Pers TH, et al. Meta-analysis of genome-wide
746 association studies identifies ten loci influencing allergic sensitization. *Nature Genetics*
747 2013;45:902-6.
- 748 101. Sleiman PMA, Wang M-L, Cianferoni A, et al. GWAS identifies four novel
749 eosinophilic esophagitis loci. *Nature Communications* 2014;5:5593.

750

751

752 **TABLES**

753 **Table 1: Major Clinical Features.** Tabulation and comparison of the clinical phenotype
 754 of patient 1 and 2.

	Patient 1	Patient 2
Genetic Workup	Heterozygous <i>STAT6</i> c.1144G>C, p.E382Q	Heterozygous <i>STAT6</i> c.1256A>G, p.D419G
Severe Atopic Disease		
Disease onset in early infancy	✓	✓
Severe, widespread treatment-resistant atopic dermatitis	✓	✓
Asthma	✓	✓
Multiple food allergies	✓	✓
Drug allergies	✓	✓
Allergic rhinoconjunctivitis	✓	✓
Infections		
Recurrent respiratory infections	✓	✓
Recurrent skin infections (e.g. <i>Staphylococcus</i> , <i>Candida</i> , <i>molluscum</i>)	✓	✓
Gastrointestinal Disorders		
Early gastro-oesophageal reflux disease (GERD)	✓	
Eosinophilic esophagitis		✓
Chronic diarrhea, protein losing enteropathy, eosinophilic infiltration, duodenal atrophy	✓	
Skeletal Issues		
Osteoporosis, pathogenic fractures	✓	
Generalized hypermobility and joint pain		✓
Vascular anomalies		
	In late 20s: Thromboembolic ischemia of 1st and 3rd toes with severe pain	Brain MRI in mid-30s (age 30-35 years) revealed multiple anatomical variants including anomalous vasculature in the circle of Willis with hypoplastic vertebrbasilar arteries, a persistent left-sided congenital trigeminal artery with tortuosity, and a hypoplastic A1 segment of the right anterior carotid artery.
	Mid-30s (age 30-35 years): Fatal spontaneous subarachnoid hemorrhage with intraventricular hemorrhage.	

Human germline STAT6 gain-of-function variants

Sharma *et al.*

Other		Adolescence (age 15-20 years): Retinal detachment in right eye
--------------	--	--

755

756

757 **Table 2. Number of published genome-wide association (GWAS) studies linking**
758 **polymorphisms (SNPs) in *STAT6* to common allergic diseases in the population.**
759 Significant genome-wide associations ($P < 5 \times 10^{-8}$) between *STAT6* SNPs and all
760 relevant allergic traits were obtained through NHGRI-EBI GWAS Catalog
761 (ebi.ac.uk/gwas/).

762

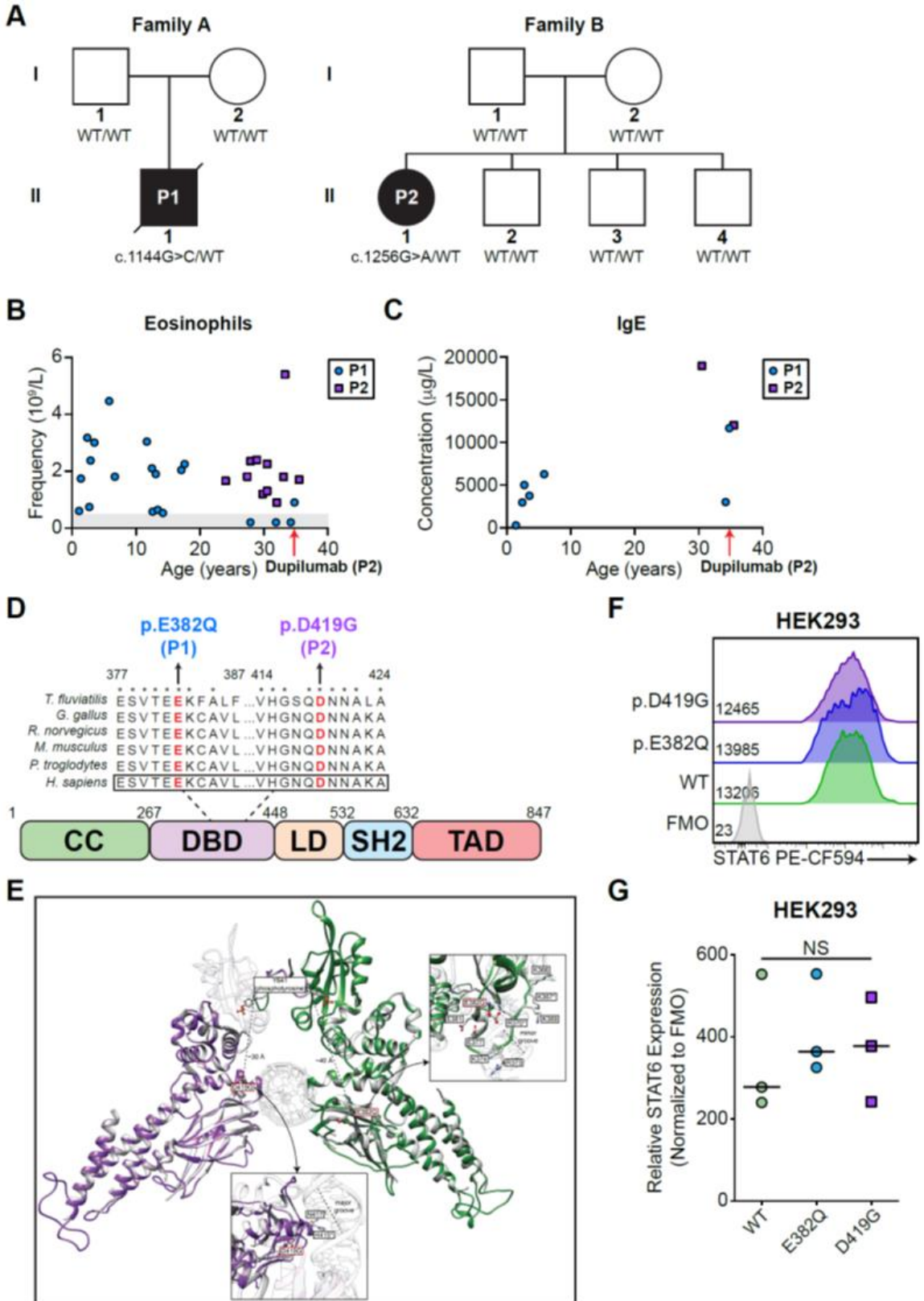
Phenotype	Number of published associations	References
Asthma*	13	76-88
Eosinophil count	6	76,89-93
Allergic disease	3	80,94,95
Atopic dermatitis/Eczema	3	81,93,96
Serum IgE level	2	97,98
Allergic sensitization	2	99,100
Allergic rhinitis	1	81
Eosinophilic gastrointestinal disorders	1	101

763 *Includes asthma, childhood-onset asthma, adult-onset asthma, and atopic asthma

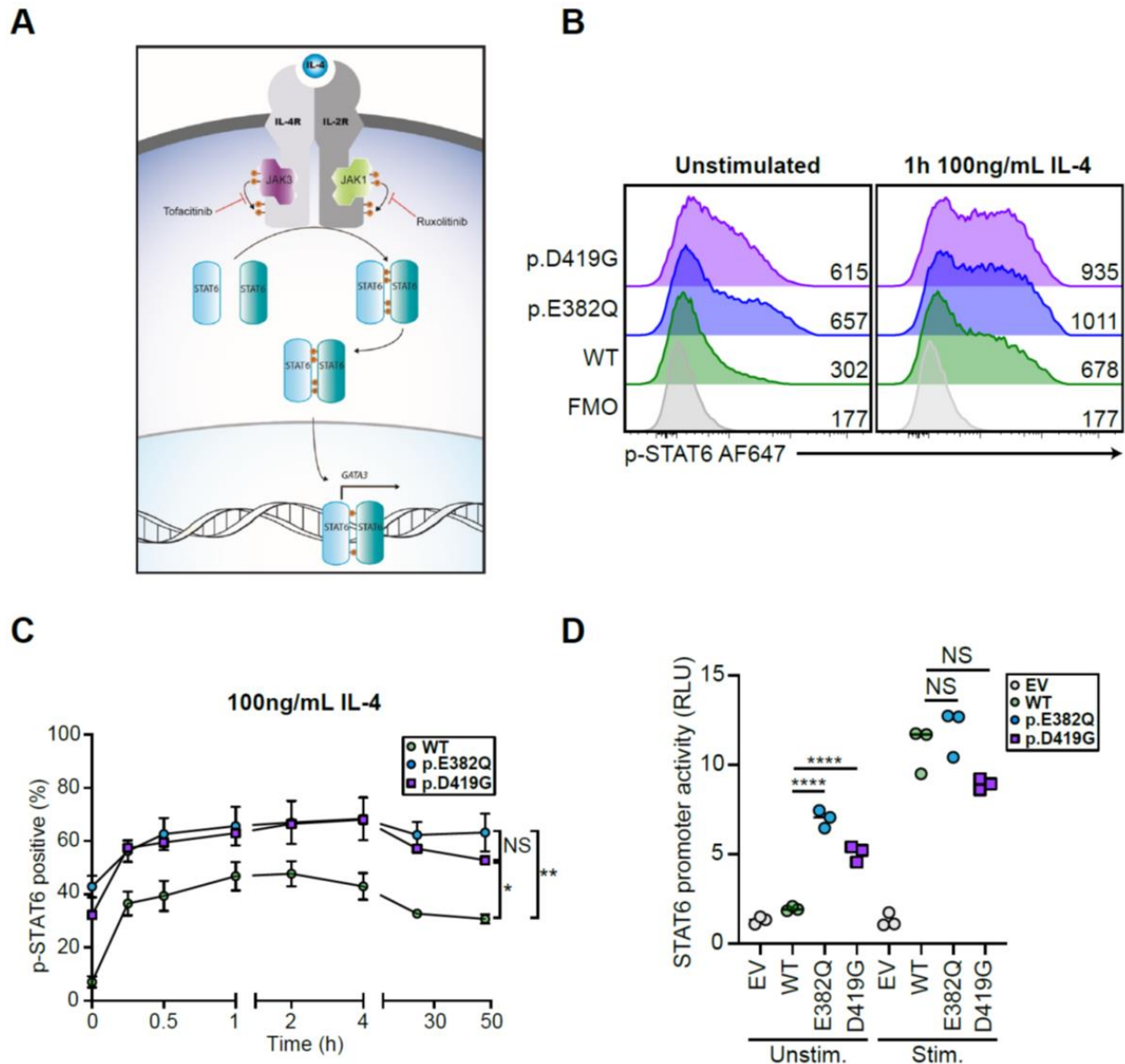
764

765

766 FIGURES



768 **Figure 1: Clinical phenotype of two patients with severe atopic disease. A)** Family
769 pedigree of the two patients. Filled symbols=affected individual, arrow=proband, unfilled
770 symbols=unaffected individual. P1 has the variant p.E382Q, P2 has the variant
771 p.D419G. **B)** Eosinophil frequency in whole blood of P1 and P2. **C)** IgE concentration in
772 whole blood of P1 and P2. **D)** Schematic illustrating the protein domains of STAT6.
773 Amino acid location of the variants shown in red. Affected region was aligned to other
774 species. Asterisks indicate full conservation. **E)** Structural model of the DNA-STAT6
775 homodimer complex. Green=p.E382, Purple=p.D419. Residues marked with an asterisk
776 (*) were demonstrated to affect the binding of STAT6 to DNA in a previous study³⁸. **F)**
777 STAT6 expression in WT-, p.E382Q-, and p.D419G-STAT6-transfected HEK293 cells.
778 **G)** Quantification of relative protein expression in F), n=3. Significance determined
779 through a one-way ANOVA and Tukey's post-hoc test.
780



781

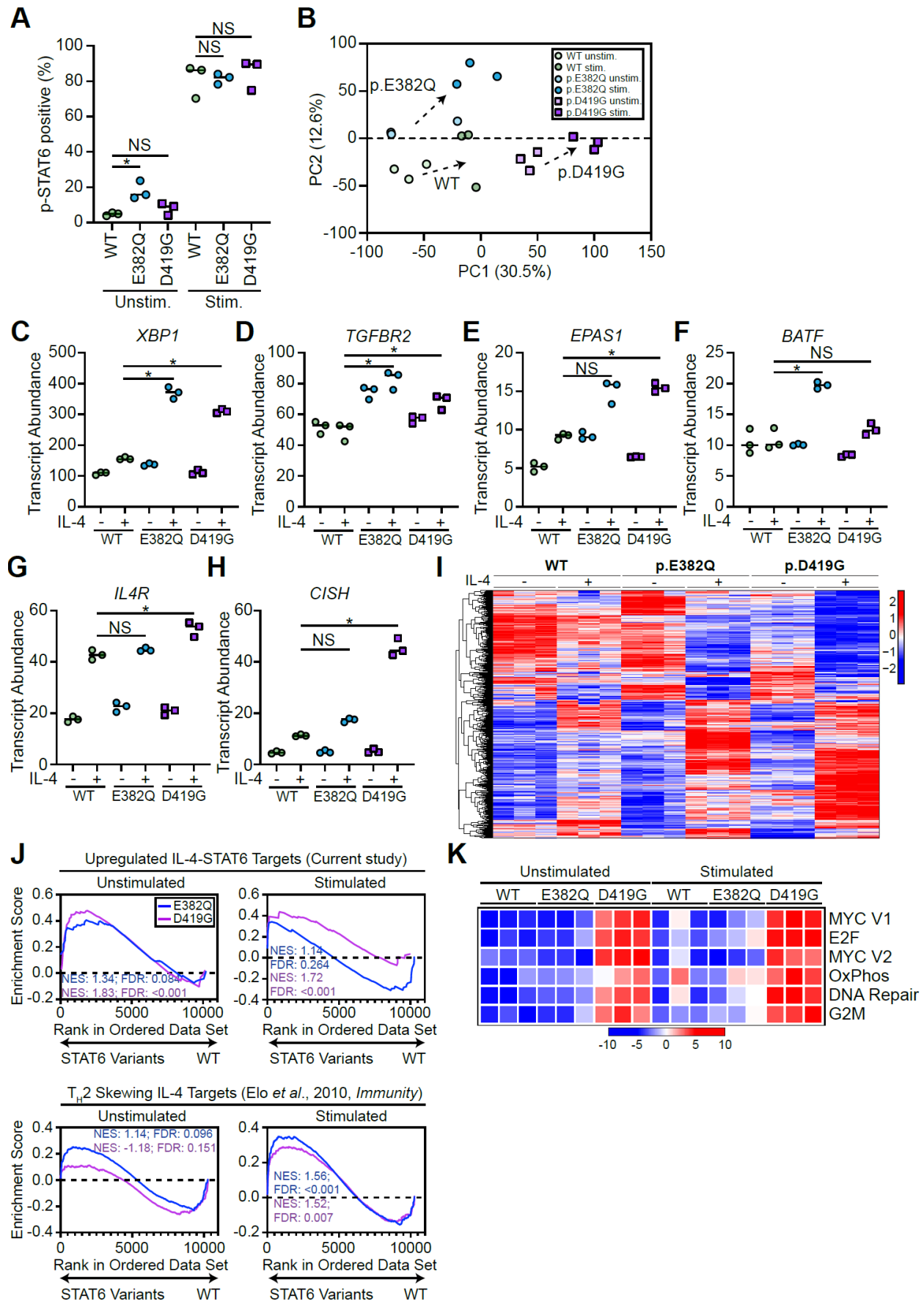
782 **Figure 2: p.E382Q and p.D419G STAT6 variants lead to increased STAT6 activity**
 783 **in HEK293 cells.** A) Schematic illustrating classical IL-4-mediated STAT6 activation,
 784 dimerization, and phosphorylation. B) Phospho-STAT6 expression in WT-, p.E382Q-,
 785 and p.D419G-transfected HEK293 cells before and after treatment with IL-4 (100ng/mL
 786 for 1h). C) Time course of phospho-STAT6-positive cells after 100ng/mL IL-4
 787 stimulation in transfected HEK293 cells, n=3. D) Luciferase assay of STAT6 activity on
 788 a plasmid containing a 4x STAT6 binding site [TTCCCAAGAA] for WT-, p.E382Q-, and
 789 p.D419G STAT6-transfected HEK293 cells before and after stimulation with IL-4

790 (100ng/mL for 4h), n=3. One-way ANOVA and Tukey's post-hoc test. *p<0.05, **p<0.01,
791 ***p<0.001, ****p<0.0001.

792

Human germline STAT6 gain-of-function variants

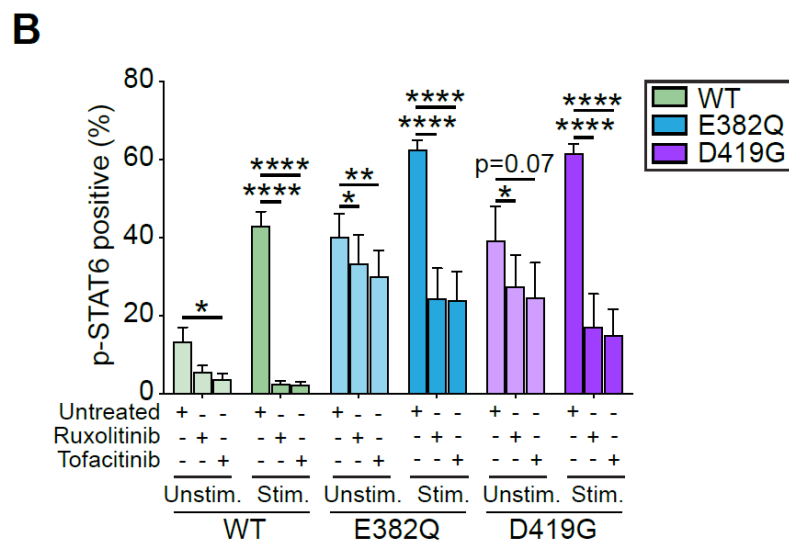
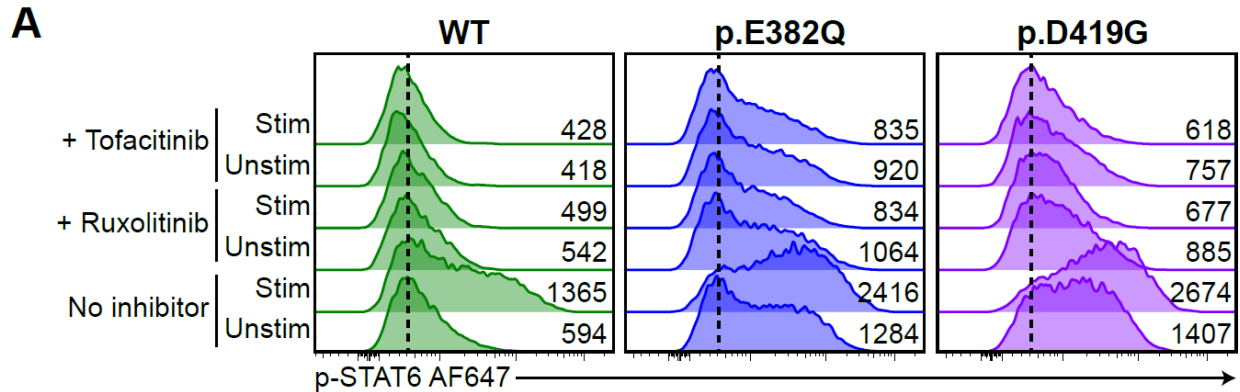
Sharma *et al.*



794 **Figure 3: p.E382Q and p.D419G STAT6 variants lead to increased STAT6 activity**
795 **in Jurkat T cells. A)** Quantification of phospho-STAT6-positive WT-, p.E382Q-, or
796 p.D419G-transduced Jurkat T cells before and after treatment with IL-4 (100ng/mL for
797 1h), n=3. **B)** Principal component analysis (PCA) comparing unstimulated and
798 stimulated (100 ng/mL IL-4 for 4 h) WT (green), p.E382Q (blue), p.D419G (purple)
799 STAT6 transduced Jurkat T cells. PC1 and PC2 contribution is shown in brackets. **C-H)**
800 Normalized counts comparing stimulated WT (green) vs. p.E382Q (blue) or p.D419G
801 (purple), for **C) XBP1, D) TGFBR2, E) EPAS1, F) BATF, G) IL4R, H) CISH. I)** Heatmap
802 representation of normalized counts of a transcription set defined as IL-4 targets in each
803 STAT6 Jurkat T cells. *adjusted P-val<0.05. **J)** GSEA plots for curated STAT6 and IL-4-
804 T_H2 targets genes, comparing WT vs. either p.E382Q (blue) or p.D419G (purple) at both
805 baseline and after stimulation with IL-4. Normalized enrichment score (NES) and
806 adjusted p-value are shown. **K)** Sample level enrichment analyses (SLEA) of
807 significantly enriched immune pathways from MSigDB Hallmark in unstimulated and IL-
808 4-stimulated samples, comparing WT vs either p.E382Q or p.D419G. Heatmap is
809 normalized across the rows and shown as relative expression.

810

811



812

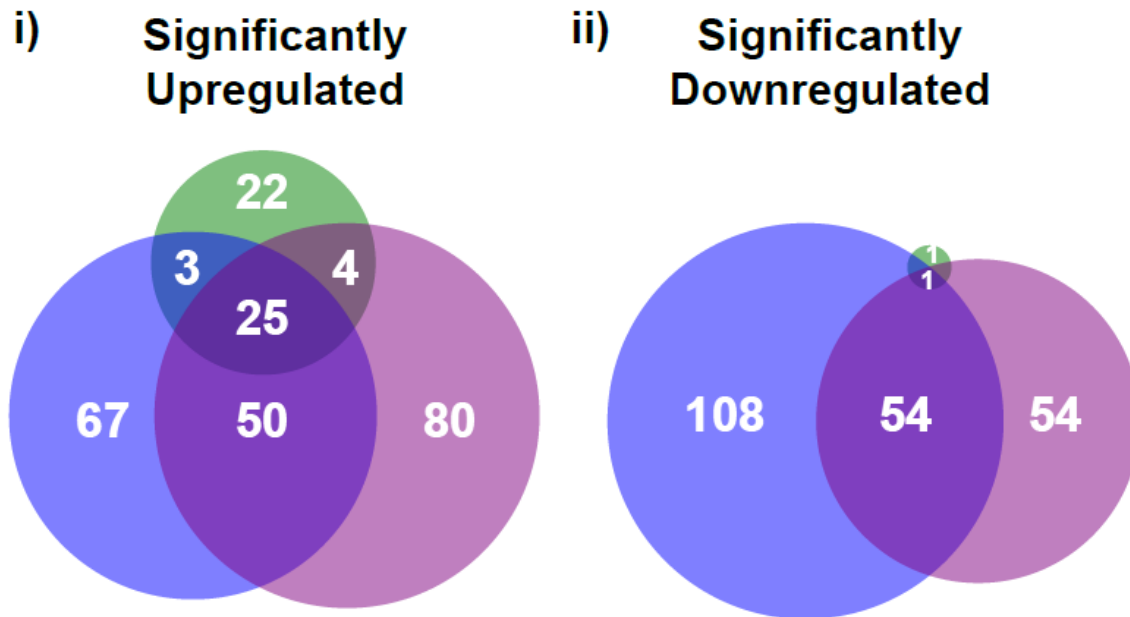
813 **Figure 4: JAK inhibitor treatment decreases gain-of-function STAT6 activity**
 814 **caused by p.E382Q and p.D419G STAT6. A)** phospho-STAT6 expression in
 815 transfected HEK293 cells pre-treated with ruxolitinib (10 μ M 2hr) or tofacitinib (4 μ M 2hr),
 816 before and after stimulation with IL-4 (100ng/mL 1h). **B)** Quantification of A), n=3. One-
 817 way ANOVA and Tukey's post-hoc test. *p<0.05, **p<0.01, ***p<0.001, ****p<0.0001.

818

819 **SUPPLEMENTAL FIGURES**

820

A



821

822

823 **Supplementary Figure 1: Extended data on STAT6 variant-transduced Jurkat T**

824 **cells. A)** Significantly upregulated (i) and downregulated (ii) genes upon IL-4 treatment
825 in WT (green), p.E382Q (blue) and p.D419G (purple) in Jurkat cells as shown via Venn
826 diagram.

827

828

829 **SUPPLEMENTAL TABLES**

830 **Supplementary Table 1:** Variant annotation and pathogenicity prediction of the variants
 831 reported in the two patients.

Variant Annotation		
	P1	P2
Chromosome	12	12
Genomic Position (GRCh37)	57498315	57496661
cDNA Position (NM_001178079.2)	1144	1256
Nucleotide Reference	G	A
Nucleotide Variant	C	G
Protein Variant (NP_001171550.1)	p.Glu382Gln (p.E382Q)	p.Asp419Gly (p.D419G)
Zygosity	Heterozygous	Heterozygous
Inheritance	<i>de novo</i>	<i>de novo</i>
dbSNP153	No entry	No entry
gnomAD (v3.1.1)	No entry	No entry
COSMIC (v95)	Somatic not reported	Somatic reported, 26 entries (COSV55668829)
<i>in silico</i> Pathogenicity Prediction Models		
CADD (v1.6)	27.7	29.3
SIFT	Deleterious (0.026)	Deleterious (0.001)
PolyPhen-2	Probably Damaging (1)	Probably Damaging (1)
LRT	Deleterious (0)	Deleterious (0)
MutationTaster	Disease Causing (1)	Disease Causing (1)
PROVEAN	Damaging (-2.71)	Damaging (-4.83)
MetaSVM	Tolerable (-0.538)	Damaging (0.610)
M-CAP	Possibly pathogenic (0.106)	Possibly pathogenic (0.294)
FATHMM MKL Coding	Deleterious (0.986)	Deleterious (0.701)

835 **Supplementary Table 2:** IL-4/STAT6 target genes in Jurkat. IL-4/STAT6 target genes
836 are shown that were either upregulated (green) or downregulated (red) in WT-STAT6
837 transduced Jurkat after stimulation with IL-4 (100ng/mL) for 4 hours.

IL4-STAT6 targets in Jurkat			
<i>SOCS1</i>	<i>STK17B</i>	<i>IRF2BP2</i>	<i>IDI1</i>
<i>MAL</i>	<i>SLC39A8</i>	<i>UBE2B</i>	<i>CHST2</i>
<i>FAM171A1</i>	<i>MZT1</i>	<i>TEX30</i>	<i>RPF2</i>
<i>CD244</i>	<i>MBNL1</i>	<i>ABCD3</i>	<i>LYPLA1</i>
<i>BCL6</i>	<i>ETS2</i>	<i>SCOC</i>	<i>CCNC</i>
<i>IL4R</i>	<i>PMAIP1</i>	<i>NDUFA5</i>	<i>CENPH</i>
<i>CISH</i>	<i>ENDOD1</i>	<i>SNX10</i>	<i>CBX3</i>
<i>RAB11FIP1</i>	<i>TMED7</i>	<i>LZTFL1</i>	<i>HINT3</i>
<i>TREML2</i>	<i>ST8SIA4</i>	<i>COX20</i>	<i>XIAP</i>
<i>SNTB1</i>	<i>PRKCQ-AS1</i>	<i>GRK6</i>	<i>CD164</i>
<i>PECAM1</i>	<i>TSNAX</i>	<i>LINC00493</i>	<i>STK17A</i>
<i>GCSAM</i>	<i>NDUFB5</i>	<i>DCK</i>	<i>DSTN</i>
<i>RASGRP1</i>	<i>XBP1</i>	<i>STAMBPL1</i>	<i>ARPC5</i>
<i>GATSL3</i>	<i>RFK</i>	<i>SGCB</i>	<i>RAP1GAP</i>
<i>FAM120AOS</i>	<i>TESPA1</i>	<i>DENR</i>	<i>CLSTN3</i>

838

839

840

841 **Supplementary Table 3:** Statistics for enrichment analysis done on Jurkat T cells,
842 comparing WT-STAT6 with either p.E382Q or p.D419G at baseline or after stimulation.

Pathways	Unstim - 1144 vs WT			Unstim - 1256 vs WT			IL4 stim - 1144 vs WT			IL4 stim - 1256 vs stim		
	NES	pval	qval	NES	pval	qval	NES	pval	qval	NES	pval	qval
MYC_V1	0.55	1	0.997	2.77	<0.0001	<0.0001	-0.93	0.638	0.608	2.81	<0.0001	<0.0001
E2F	1.04	0.364	0.61	2	<0.0001	<0.0001	1.18	0.113	0.429	2.98	<0.0001	0.001
MYC_V2	-1.23	0.157	0.253	2.01	<0.0001	<0.0001	-1.53	0.017	0.044	2.02	<0.0001	<0.0001
OXPPOS	1.4	0.007	0.156	1.82	<0.0001	0.003	-0.71	0.98	0.942	1.43	0.008	0.069
DNA repair	1.01	0.409	0.622	1.63	<0.0001	0.016	0.66	1	0.976	1.39	<0.0001	0.069
G2M	0.68	0.998	1	1.49	<0.0001	0.043	0.86	0.825	0.93	1.77	<0.0001	0.009

843